32. THE CLAYSTONE LAYER BETWEEN TWO BASALT FLOWS IN HOLE 432A: AN ARGUMENT FOR THE EMERGENCE OF NINTOKU SEAMOUNT

Anne Marie Karpoff, Institut de Géologie, Strasbourg, France

INTRODUCTION

One argument for the subaerial formation of Nintoku Seamount in the Emperor chain is the occurrence of a red claystone interlayered between two basalt flows in Hole 432A. Detailed study of this material, presented here, defines its nature and composition and strongly indicates its subaerial formation.

STRATIGRAPHIC POSITION AND LITHOLOGIC DESCRIPTION

The red claystone underlying the uppermost two flow units, which are moderately altered alkalic basalts, occurs in the bottom of the core-catcher sample of Core 2 (432A-2, CC, 20–30 cm). This claystone overlies Flow Unit 3, another alkalic basalt with an oxidized top. The 10-cm-thick claystone has three major parts, differentiated by color and texture (Figure 1). The upper part of the material (20 to 23 cm) at the contact with Flow Unit 2 is a yellowish red (5YR 4/6) sandy claystone. This sandy layer changes gradually to a dark reddish brown (2.5YR 3/4) claystone (23 to 26 cm). On the bottom (26 to 30 cm), the sandy claystone is dark brown (7.5YR 3/2) and heterogeneous. The lower part is deformed, probably by drilling.

METHODS

Mineralogical and chemical analysis followed the methods of the Institut de Géologie in Strasbourg (France), as described in this volume by Karpoff and others.

STRUCTURE AND MINERALOGY

A thin section made from the upper part of the red sandy claystone shows fragments of volcanic detritus and phenocrysts such as olivine and feldspars. The matrix is composed of clays and iron oxides which often occur in fine oriented layers. This deposition of the small particles may indicate sub-horizontal deposition of the primary material. Feldspars and olivine (iddingsite) are altered; the iron-titanium minerals, such as titanomagnetite, are well preserved. The vesicles are fringed by chalcedony, which sometimes forms spherules in the altered olivine mass or the clay matrix (Figure 2).

The SEM observations on the red part of the claystone confirm the orientation of the hematite and clay particles seen in the thin section, and show rounded spherules of chalcedony (Plate 1, Figure 1) and magnetite crystals (Plate 1, Figure 2).

Mineralogical analysis of the bulk material and the clay fraction (<2 μm), using X-ray diffraction techniques on the two most dissimilar samples, shows that the red level (23 to 25 cm) contains hematite, magnetite, titanomagnetite, traces of rutile, and cryptocrystalline silica. The clay fraction is composed of kaolinite and traces of smectites. In the brown level (27 to 29 cm), rutile, olivine, plagioclase, cryptocrystalline silica, and traces of goethite occur. The clay fraction comprises kaolinite and abundant smectites.

The TEM observations of the clay fraction indicate that it is composed of kaolinite and spheroidal or squat cylindrical halloysite (Plate 1, Figures 3 and 4). Halloysite is a typical fast-forming mineral in soils from volcanic deposits, and particularly in young soils. Air-dried or low-temperature-dried halloysite collapses to the same X-ray diffraction spacing (7.2Å) as kaolinite, and has the same chemical composition. A complete review of the occurrence, formation, and evolution of these clays minerals in young soils from volcanic materials, was presented by Dixon and Weed (1977). The cylindrical structure of halloysite is described by Kirkman (1977).

GEOCHEMISTRY

The results of the chemical analysis, made on the bulk material from two levels, as above, are given in Table 1.

The Red Level (23 to 25 cm)

The composition of the upper part of the claystone can be established quantitatively. Assuming that the theoretical formula of kaolinite is 39.5 per cent Al_2O_3, 46.5 per cent SiO_2, and 14.0 per cent H_2O, and that the Si/Al ratio is 1.04, the sample contains about 62.5 per cent kaolinite, 3 per cent silica (chalcedony), 28 per cent iron-titanium oxides (such as ilmenorutile, magnetite, and titanomagnetite), and 6.5 per cent other silicates (smectites, feldspars, etc.). In this case, the loss on ignition is the water content of kaolinite. This part of the red claystone contains very little water. Trace elements (V, Cr, etc.) are principally associated with the iron-titanium oxides.

The Brown Sandy Level (27 to 29 cm)

The chemical composition of the lower part of the claystone is in harmony with its mineralogical components. The K_2O, Na_2O, and Ba contents correspond to feldspars, and MgO to the smectites. The values of ratios of V, Pb, Cu, Ni, and Co to the Fe_2O_3 content are lower than similar ratios for the uppermost level. The Fe/Ti ratio is also lower, and can be explained by the low concentration of free iron oxides. It is not possible

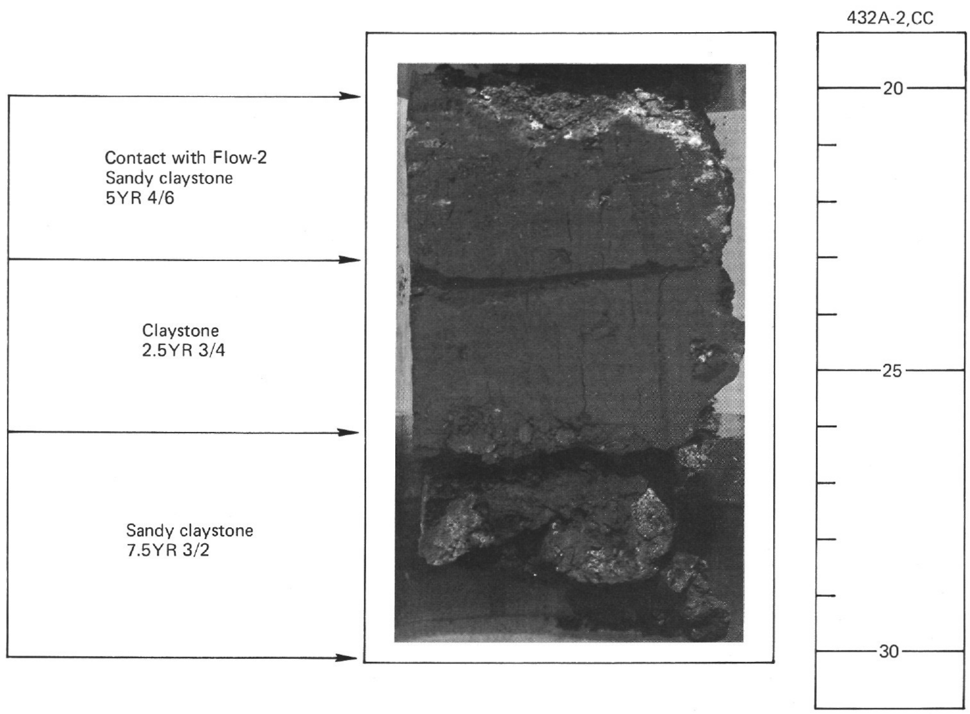

Figure 1. *The red level interlayered between basalt Flow Units 2 and 3, Hole 432A, Nintoku Seamount.*

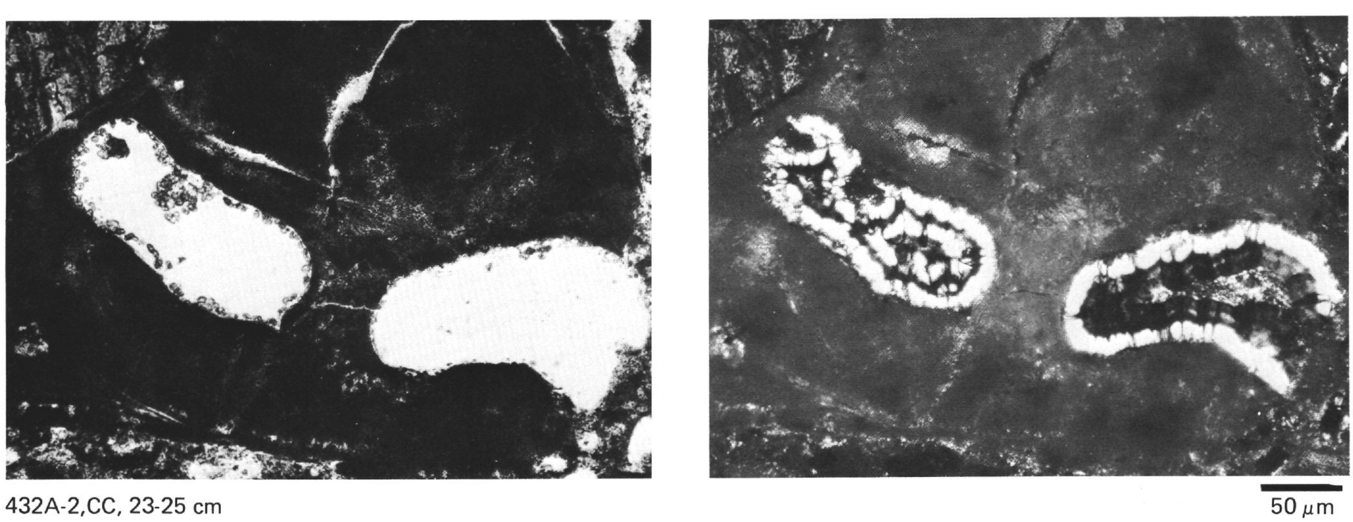

Figure 2. *Thin section of the sandy upper part of the red layer. Alveole fringed by chalcedony in red altered olivine (iddingsite). 1-Natural light; 2-polarized light.*

TABLE 1
Chemistry of Two Samples of the Red Weathered Layer, Hole 432A, Nintoku Seamount

	2,CC,23-25 cm	2,CC,27-29 cm
Major-Element Oxides (%)		
SiO_2	32.6	41.9
Al_2O_3	25.0	20.7
MgO	0.87	1.50
CaO	0.5	1.3
Fe_2O_3	24.2	17.4
Mn_3O_4	0.266	0.231
TiO_2	4.08	3.71
Na_2O	1.02	2.42
K_2O	1.32	1.97
IGN	8.74	6.88
Total	98.60	98.01
Trace Elements (ppm)		
Sr	143	107
Ba	103	233
V	447	286
Ni	115	62
Co	74	63
Cr	117	117
B	229	151
Zn	283	303
Ga	45	44
Cu	175	53
Pb	364	206
Ratios		
Si/Al	1.15	1.78
Na_2O/K_2O	0.77	1.23
Mn/Fe	0.011	0.014
Fe/Ti	6.9	5.4
V/Fe	26.4	23.5

to calculate precisely the quantitative composition of this part of claystone, because of its diversified mineral assemblage. The feldspars make up about 30 per cent and clays about 10 per cent of the brown sandy level. This level appears impoverished in Si, Mg, Ca, and K, but enriched in Fe and Ni compared with the lower basalt flow (Sample 432A-3-2, 106-108 cm: chemical analysis from the shipboard report).

INTERPRETATION AND DISCUSSION

The mineralogical and geochemical composition of the red level is like that of a soil formed on land by weathering of volcanic material. Such soils are andosols or, less likely, latosols or lateritic soils. This is illustrated by extensive literature on soils from the Hawaiian Islands and volcanic regions bordering the Pacific Basin or on soils derived from ash deposits and basalts by tropical or sub-tropical weathering (Sherman et al., 1948; Sherman, 1950; Segalen, 1957; Patterson and Roberson, 1961; Correns, 1962; Loughnan, 1969; Colmet-Daage et al., 1970; Leonvallejo and Segalen, 1970; Cortes and Franzmeier, 1972; Mohr et al., 1972; Gibert, 1973; Dixon and Weed, 1977). The red claystone facies differs also from oceanic volcanosedimentary sequences in surface sediments, such as those described by Hoffert et al. (1978). Deep-sea authigenic silicates in a volcanic environment are generally smectites and zeolites associated with ferromanganese oxyhydroxides.

Nevertheless, the thickness (very thin) and the structure (absence of well-defined pedologic horizons) do not permit me to conclude that this red sandy claystone is a typical soil, in the strict definition of the term. But the structure of the clay assemblage and iron-oxide matrix, and the mineralogical bulk composition, agree better with the hypothesis that this facies results from weathering of a fine-grained layer of pyroclastic volcanic material or tuffaceous ash. This soil developed in a short time, and its development did not end with formation of a typical andosol or lateritic soil, because it experienced a subsequent thermal transformation. This secondary evolution of the thin soil layer resulted from deposition of the upper basalt Flow Unit 2. This volcanic action induces successive thermal effects, more marked in the upper part of the weathered layer. These effects are (1) dehydratation and crystallization of iron hydroxides to hematite; (2) stabilization of the clays, especially the kaolinite; (3) formation of chalcedony; and (4) mobilization of calcium and potassium by steam and hot water. A similar evolution (in the red levels from Coirons, France) has been described by Moinereau et al. (1972).

The contact between the red soil and the upper basalt flow is also characterized by rare altered volcanic detritus and of phenocrysts enclosed in the clay and hematitic matrix. A schematic diagram for the formation of the red weathered layer of Hole 432A is given in Figure 3.

From its stratigraphic position, the red weathered level is approximately upper Paleocene. The K/Ar and $^{40}Ar/^{30}Ar$ age of the upper part of the underlying basalt Flow Unit 3 is 56.2 ± 0.6 m.y. (Dalrymple et al., this volume). The volcanic sands above the overlying basalt Flow Unit 2 are Paleocene (Butt, this volume). The short interval of time between deposition of these vol-

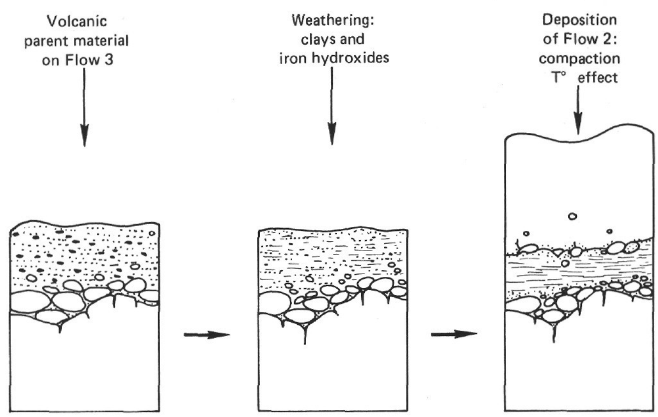

Figure 3. *Schematic evolution of the red weathered level, Hole 432A, Nintoku Seamount. 1-Deposition of basaltic tuffaceous ash on top of basalt Flow Unit 3. 2-Weathering of the volcanic material, with formation of clays and iron hydroxides. 3-Deposition of the basalt Flow Unit 2, inducing compaction and low-temperature transformation of the upper part of the red weathered soil layer.*

canic and sedimentary facies agrees with the fast weathering of the volcanic parent material to form the red soil.

OTHER OCCURRENCES OF RED FORMATIONS INTERLAYERED TO BASALTS

Other examples of red formations interlayering basalts have been observed and studied elsewhere. In the Atakor Massif of Africa, the red level is developed between ash and phonolites (Bordet, 1951); in Cameroun it is below ash deposits; and in Hoggar, it is between ash and basalt flows (Leprun, personal communication). In the Massif Central of France, red formations exist between quaternary basaltic flows at Aurillac and Coirons (Moinereau et al., 1972; Gibert, 1973).

CONCLUSIONS

The red claystone interlayered between basalt flows of Hole 432A is a subaerial formation. From its structure and mineralogical and geochemical composition, I conclude that it was formed by weathering of a basaltic tuffaceous ash under subtropical conditions and afterwards underwent a low-thermal transformation when the upper basalt flow settled. This agrees with the hypothesis that the Emperor seamounts, and in particular the Nintoku Seamount, were emergent during the period of their formation and of successive deposition of basalt flows.

ACKNOWLEDGMENTS

I thank J. C. Leprun and M. Hoffert for helpful discussions. The electron microscope investigations (SEM and TEM) were made with I. Peterschmitt and D. Trauth.

REFERENCES

Bordet, P., 1951. Présence de laterite fossiles dans l'Atakor du Hoggar, *C.R. Soc. géol. France,* t. 1, p. 97.

Colmet-Daage, F., Gautheyron, J. et M., Dekimpe, C., Siefferman, G., Delaune, M., and Fusil, G., 1970. Caractéristiques de quelques sols dérivés de cendres volcaniques de la côte pacifique du Nicaragua, *Cah. ORSTOM sér. Pédol.,* v. VIII, p. 113–172.

Correns, C. W., 1962. Observation sur la formation et la transformation de minéraux argileux lors de la décomposition des basaltes. *Colloque Int. C.N.R.S. No. 105. Genèse et Synthèse des Argiles,* Paris, 1961, p. 116-121.

Cortes, A. and Franzmeier, D. P., 1972. Weathering of primary minerals in volcanic ash-derived soils of the Central Cordillera of Columbia, *Geoderma,* v. 8, p. 165-176.

Dixon, J. B. and Weed, S. B., 1977. Minerals in soil environments, *Soil Sci. Soc. Am.,* p. 948.

Gibert, J. P., 1973 Mise en évidence d'une altération de type ferralitique au Miocène terminal du Sud du Cantal, *C.R. Acad. Sci. Paris,* t. 277, p. 545-547.

Hoffert, M., Karpoff, A. M., Clauer, N., Schaaf, A., Courtois, C., and Pautot, G., 1978. Néoformations et altérations dans trois faciès volcanosédimentaires du Pacifique Sud, *Oceanologica Acta,* v. 1-2, p. 187-202.

Kirkman, J. H., 1977. Possible structure of halloysite disks and cylinders observed in some New Zealand ryolitic tephras, *Clays Minerals,* v. 12, p. 199-215.

Leonvallejo, G. and Segalen, P., 1970. Observations sur des sols rouges dérivés de roches volcaniques basiques dans le Bafio (Mexique Central), *Cah. ORSTOM sér. Pédol.,* v. VIII, p. 49-62.

Loughnan, F. C., 1969. *Chemical Weathering of the Silicate Minerals:* New York (Elsevier Publ. Company), p. 154.

Mohr, E. C. J., Van Baren, F. A., and Van Schuylen-Borgh, J. *Tropical Soils:* Mouton-Ichtiar Bare and Van Hoere Ed., p. 481.

Moinereau, J., Grillot, J. C., and Naud, G., 1972. Origine et géochimie des niveaux rouges du plateau basaltique des Coirons en Ardèche, *Rev. Géo. phys. et Géol. dyn.,* v. XIV, p. 85-94.

Patterson, S. H. and Roberson, C. E., 1961. Weathered basalt in Eastern part of Kanai, Hawaii, *USGS Prof. Paper,* v. 424C, p. 195-198.

Segalen, P., 1975. Etude des sols dérivés de roches volcaniques basiques à Madagascar, *Mém. Inst. Scientifique de Madagascar,* ser. D, t. VIII, p. 1-81.

Sherman, G. D., 1950. Hawaiian ferruginous laterite crusts, *Pacific Sci.,* v. 4, p. 315-322.

Sherman, G. D., Foster, Z. C., and Fujimoto, C. K., 1948. Some of the properties of the ferruginous hermic latosols of the Hawaiian Islands, *Soil. Sci. Soc. Am. Proc.,* v. 13, p. 141-146.

PLATE 1

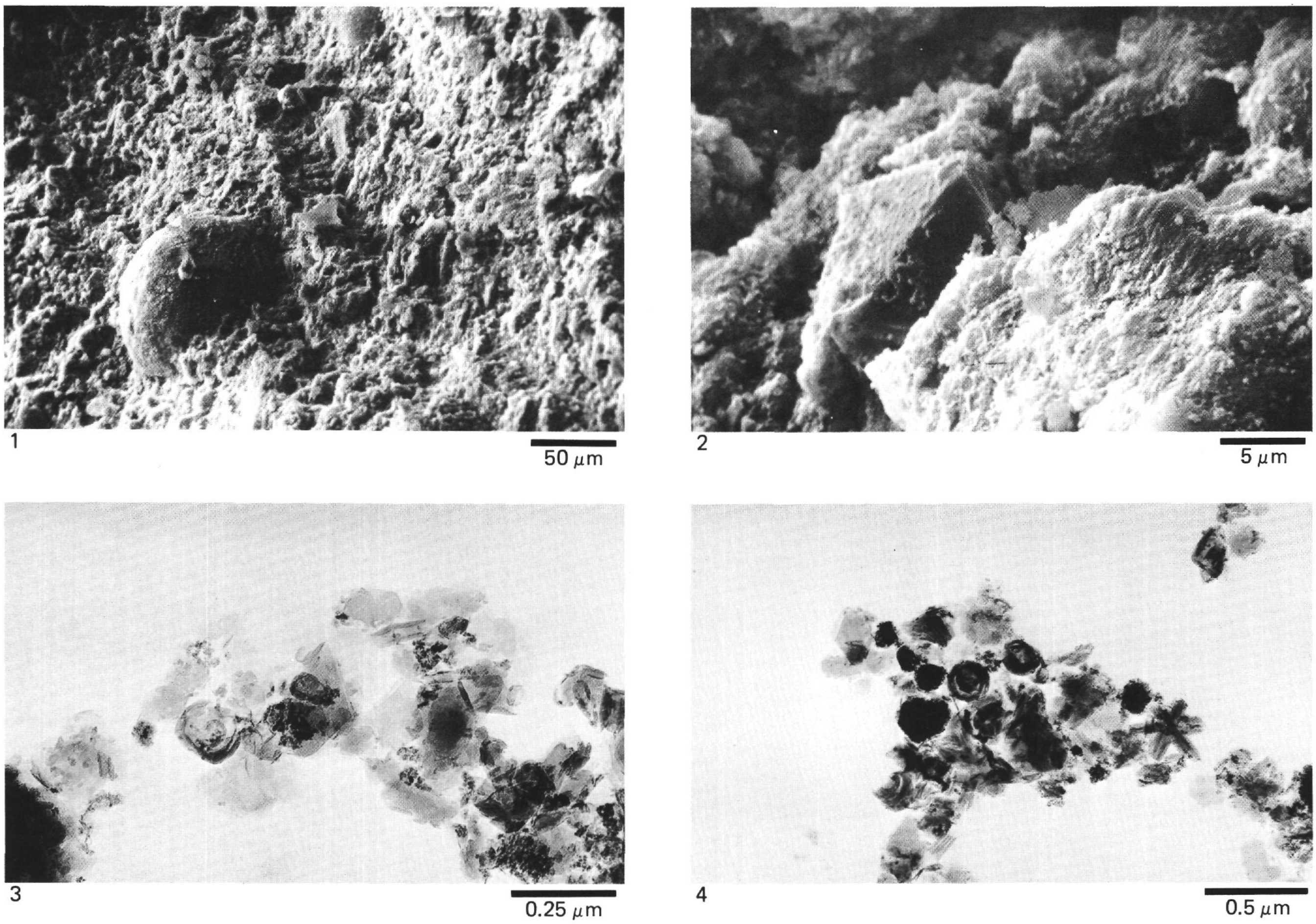

PLATE 1

SEM AND TEM photomicrographs of the Red Claystone Interlayered between Basalt Flows (432A-2, CC, 23-25 cm).

Figure 1	The fine zonation of clay and hematic mass is visible; enclosed spherule of chalcedony (SEM).
Figure 2	A well-crystallized magnetite mineral in the clay and hematitic matrix (SEM).
Figure 3	TEM photomicrograph of the clay fraction from the red level; the hexagonal plates are kaolinite and the squat cylinders are halloysite.
Figure 4	TEM photomicrograph of the clay fraction from the red level, composed of kaolinite, squat cylindrical halloysite, and goethite.